BENTHIC COVERAGE AND BOTTOM TOPOGRAPHY OF CORAL REEF ENVIRONMENT

Ashwin Gujrati[1*], Shard Chander[1] and Mohit Arora[1]

[1]Space Applications Centre, Indian Space Research Organisation, Ahmedabad, India

[*]Corresponding author email: ashwin8199@sac.isro.gov.in

KEY WORD: Remote sensing, Hyperspectral, AVIRIS-NG, Atmospheric correction

ABSTRACT: Remote sensing measurements in coral reef environments commonly confront the problem of overlying atmosphere and modification of spectral signal due to water column over the bottom substrates. In order to correct these problems, hyperspectral observations offer an advantage over multispectral observations. This study was carried out with an objective to map benthic coverage and bottom topography over Pirotan reef in Gulf of Kachchh region (Gujarat), India. Airborne hyperspectral remote sensing data from Airborne Visible Infrared Imaging Spectrometer- Next Generation (AVIRIS-NG) sensor was acquired during low tidal condition with an average flight altitude of 8km on 14th Feb 2016 at Pirotan reef for mapping the benthic coverage and the bottom topography. The methodology involved atmospheric correction, simultaneous retrieval of water parameters, bathymetry, water column correction and mapping. Atmospheric correction was performed by removing path radiance and aerosol contribution and dividing by atmospheric transmittance and incoming solar irradiance to obtain remote sensing reflectance. Model derived error minimization technique was used for simultaneous retrieval of water parameters and bathymetry. Derived water parameters were used to account for water column attenuation and retrieve concomitant true bottom signature. Increased classification accuracy for coral reef mapping was achieved. Mapping is one of the most common applications associated with the remote sensing of coral reefs and benthic coverage.

INTRODUCTION:

Remote sensing data over water measures radiance that originates from sunlight that passes through the atmosphere, is reflected, absorbed, and scattered by constituents in the water bodies, and is transmitted back through the atmosphere to the sensor. The outgoing radiance from the water surface is contribution of both radiances from the water column and from the bottom substrate (in case of shallow waters). Water leaving radiance from the water column is contribution of both physical and biological parameters of water through inherent optical properties (IOP's). Most fundamental IOP's are spectral absorption coefficient and total scattering coefficients (Morel 1995). Contribution from the bottom substrate is affected by the overlying water column along with the water quality parameters. Hence coral reefs become a complex environment for parameter estimation.
In order to map coral reef environments for its highly complex water type and relatively small horizontal spatial scales, high spatial and spectral resolution data is required. Mapping of the fine-scale variability will improve characterization of habitat, both for corals and for various species living in the reefs. Mapping of coral reefs and other benthic substrates requires information of water depth and water quality. Water column information with water quality parameters is useful in estimating bottom coverage spectra by removing effect of overlying water column from the benthic substrates (Mumby *et al.*, 1998).

With advances in the growth of hyperspectral data many analytical and semi-analytical algorithm have been developed for retrieval of bathymetry and water quality parameters for optically complex waters (Odermatt *et al.*, 2012). Maritorena (1994) derived diffuse reflectance of oceanic shallow water using a set of simplifying assumptions of replacing different attenuation coefficient with diffuse attenuation coefficient. Gege (2012) developed an analytic model for the direct and diffuse components of the downwelling irradiance in the water column. Giardino *et al.* (2012) developed a software package incorporating their Bio-Optical Model Based tool for Estimating water quality and bottom properties from Remote sensing images (BOMBER). Brando *et al.* (2003, 2012) present an adaptive implementation of the linear matrix inversion (LMI) method which accounts for variability in both IOPs and mass-specific IOPs (SIOPs) over space and time in wide-ranging optically-complex waters. More sophisticated neural network and physics-based inversion methods have also been used to estimate in-water inherent optical properties (IOPs) (Odermatt *et al.*, 2012). Salama and Verhoef (2015) present a new, forward model analytical inversion solution ("*2SeaColor*") for the retrieval of the depth profile of the downwelling diffuse attenuation coefficient.

This study used a reef-up approach to map benthic substrates, bathymetry and water column information on Pirotan Reef, using a simple inversion model. This study was achieved by measuring *in-situ* pure end-member spectral signatures, processing them to be compatible with AVIRIS-NG image data and using them to supervise image classification.

STUDY AREA:

Gulf of Kachchh (22° 15' N to 23° 40' N Latitude and 68° 20' E to 70° 40' E Longitudes) is very rich in terms of biodiversity value and supports varied coastal habitats including coral reefs, mangroves, creeks, mud flats, islands, rocky shores, sandy beaches, etc. (Fig. 1). It is situated at the northern boundary of Saurashtra Peninsula of Gujarat state of India. The coral reef region of Gulf of Kachchh represents the northern most limit of coral reefs in India. One third of Indian hard (Scleractinian) coral genera is found in Gulf of Kachchh region (Venkataraman, 2011). The test reef or Pirotan reef is northernmost fringing reef in protected zone of Gulf of Kachchh Marine National Park and Sanctuary. Pirotan reef is located between 22° 34' N and 22° 38' N Latitudes and 69° 55' E and 69° 59' E Longitudes with total area coverage of 12.9 km^2. The benthic substrates like Favia, Green algae, Brown algae, Seagrass, Sand, Sargassum, Silt, Mangrooves etc. have been identified through *in-situ* collected spectral reflectance data. Gujarat coast of India is a macro-tidal environment marked with semi-diurnal tidal desiccations (Navalgund *et al.*, 2010). The oceanic waters in coast of Gujarat is highly turbid and make it nearly invisibile to map coral reef bathymetry with overlying seawater. These reefs are exposed only in low tidal condition and maximum exposure is found in yearly, equinoctial spring tides resulting in negative low tides facilitating *in situ* reef measurement with virtually no water column.

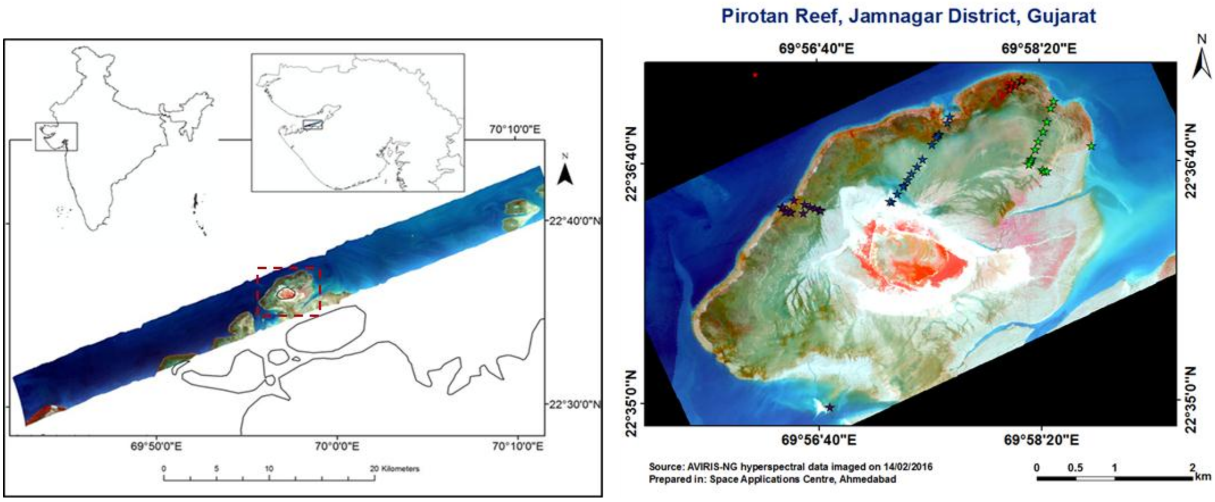

Figure 1: AVIRIS-NG Hyperspectral data and field data collection over the Pirotan reef, Gulf of Kachchh, region, Gujarat. Star point in different colour shows in-situ spectra taken during period from 12^{th} -15^{th} February, 2016

DATA USED:

In-situ spectra measurements were collected from 12^{th} to 15^{th} February 2016, with Analytical Spectral Devices (ASD) Fieldspec3 and Spectra Vista Corporation (SVC) HR 1024 spectroradiometer. These spectroradiometer is compact, field-portable, precision instrument with a spectral range of 350-2500 nm and a rapid data collection time of 0.1 second per spectrum (FieldSpec® 3 User Manual, 2006). All substrates reflectance measurment were accomapined by the measuments of the downwelling irradiance reflected from a Spectralon (calibrated in a laboratory against a Spectralon standard) or white plate also known as Teflon panel (Kutser *et al.*, 2006). The subsrates reflectance was then calculated as a ratio of radiance from the subsrates against the downwelling irradiance reflected from the white plate. The total number of reflectance of benthic substrates was collected about 52.

Airborne Visible Infrared Imaging Spectrometer – Next Generation (AVIRIS-NG) data with field-of-view 0.1 micro radian imagery became available from airborne platform, providing a new resource for the development of mapping and monitoring programs for coral reefs in remote locations. AVIRIS-NG hyperspectral data was collected from Beechcraft B-200 flying at approx. 6.8 km altitude on 14 February, 2016 at 07:05:14 hrs GMT. Data acquisition time was optimised at low tide period to get the maximum exposure of the reef above mean sea level to study the coral reef habitat zonation. AVIRIS-NG data contains 598 cross track samples and 425 bands from 370 to

2510 nm with Full Width Half Maximum (FWHM) of 5.5 to 6 nm, 7.8 meters' spatial resolution and 32-bit radiometric resolution radiance data in μW/sr/nm/cm^2. Pre-processing correction converted radiance values to remote sensing reflectance.

METHODOLOGY:

Atmospheric correction is the most critical as well as important steps in hyperspectral remote sensing. The water leaving radiance is scattered and absorbed by overlying atmosphere and alters the spectral signature of remote sensing reflectance of water. Atmospheric correction for hyperspectral data requires very accurate modelling of scattering and absorption effects in the atmosphere. Radiance measured (Ls) at the sensor level is total contribution from Aerosol (La), Rayleigh (Lr) path radiance and water leaving radiance (Lw) after transmittance through atmosphere (t), can be expressed as (Gordon *et al*. 1997).

$$Ls = La + Lr + t\ Lw \tag{1}$$

Rayleigh path radiance (Lr) was calculated and removed using Bucholtz 1994. Assuming deep clean water has negligible reflectance in NIR region, two narrow channels (912 nm and 1012 nm) were used to calculate aerosol optical thickness and then extrapolated to all hyperspectral bands by calculating Armstrong exponent. After removing both atmospheric path radiance i.e. aerosol and Rayleigh path radiance, the remaining radiance is water leaving radiance at the sensor. Water leaving radiance at the sensor is then divided by atmospheric transmittance (t) calculated using total Rayleigh and aerosol contribution in the atmosphere. The derived water leaving radiance is then divided by incoming extra-terrestrial solar irradiance (Es) to get above-surface remote-sensing reflectance (R_{rs}).

$$Lw = (Ls - La - Lr) / t \tag{2}$$

$$R_{rs} = Lw / Es \tag{3}$$

The approach of Lee *et al*. (2002) is used to derive the inherent optical properties of the coastal waters. This methodology uses different steps; in the first step, the above surface remote sensing reflectance (R_{rs}) would be converted to below surface remote sensing reflectance (r_{rs}) because satelilites and many other sensors measure remote sensing reflectance from above the surface. Remote sensing reflectance below surface (r_{rs}) is a function of the absorption and backscattering coefficients.

For the R_{rs} to r_{rs}conversion (Gordon *et al*., 1988),

$$r_{rs} = \frac{R_{rs}}{0.5+1.7R_{rs}} \tag{4}$$

Below-surface spectra r_{rs} is sum of remote sensing reflectance from optically deep water $r_{rs}^{deep}$and remote sensing reflectance from the bottom substrate r_{rs}^{bot}.

$$\mathrm{r_{rs}} = r_{rs}^{deep} + r_{rs}^{bot} \tag{5}$$

$$r_{rs}^{deep} = f\frac{b_b}{a+b_b} \tag{6}$$

$$r_{rs}^{bot} = (A - r_{rs}^{deep})\exp(2kH) \tag{7}$$

Remote sensing reflectance from optically deep water r_{rs}^{deep} is computed by IOP's. Reflectance of deep water just below the water surface is relation with water parameters absorption a (λ) and backscattering coefficients b (λ). Where f is proportionality factor. Remote sensing reflectance from the bottom substrate r_{rs}^{bot} is given by Maritorena 1994. A is albedo of bottom substrate which is fractional sum of fractional coverage of different bottom type.

$$a(\lambda) = a_w(\lambda) + Ca_c^*(\lambda) + Ya_Y^*(\lambda) \tag{8}$$

$$b_b(\lambda) = b_{b,W}(\lambda) + C.b_{b,C}^*. + C_S.b_{b,S}^*.\left(\lambda/_{\lambda_S}\right)^n \tag{9}$$

Absorption of water constituents is the sum of the components' absorption coefficients. Three groups of absorbing water constituents are considered: natural water, phytoplankton and gelbstoff/CDOM. Absorption by pure water $a_w(\lambda)$ (m^{-1}) is a combination from different source (304-386 nm: Lu (2006); 387.5-710 nm: Pope & Fry (1997); 712.3-1838 nm: Kou *et al*. (1993)). High number of phytoplankton species that occur in natural waters causes some variability in phytoplankton absorption properties. Specific absorption coefficient $a_c^*(\lambda)$ used as weighted sum of five spectra and represents a mixture which can be considered as typical for Lake Constance calculated by Heege (2000). Gelbstoff absorption is the product of concentration 'Y' and specific absorption $a_Y^*(\lambda)$ calculated using the usual exponential approximation (Nyquist 1979; Bricaud *et al.* 1981): $a_Y^*(\lambda) = \exp[-S \times (\lambda - \lambda_0)]$, where S denotes the spectral slope. Default values: λ_0=440 nm and S=0.018 nm^{-1}.

Backscattering $b_b(\lambda)$ is the sum of backscattering by pure water, chlorophyll and suspended matter. Backscattering due to water is calculated as $b_{b,W}(\lambda)$ = $b_1(\lambda/\lambda_1)^{-4.32}$; where b1=0.00111 m^{-1} for fresh water and b1=0.00144 m^{-1} for oceanic water and λ_1=500 nm. Backscattering by chlorophyll particles is calculated as: $b_{b,C}^* = 0.0006 * C^{-0.37}$ Back scattering due to suspended particles is calculated with $b_{b,S}^*$=0.0042, λ_S=500 and n=1 (Buiteveld *et al.*, 1994; Gege P., 2014).

Using above empirical and semi analytical equations, remote sensing reflectance of water can be calculated as a function of chlorophyll concentration, CDOM concentration, suspended sediment concentration, water column depth and fractional coverage of bottom type (see Fig. 2).

$$\mathrm{r_{rs}} = f\left(C_{Chl}, C_{CDOM}, C_{SSC}, f_{sand}, f_{algae}, H\right) \tag{10}$$

With the use of hyperspectral data, we get many equations (# wavelength) for above mentioned 6 unknowns. To solve the above set of equation we have used least square error minimization techniques. To keep the variable values within the range we have fixed the equations at bound of maximum and minimum values.

RESULTS AND DISCUSSIONS:

The atmospheric correction was performed assuming deep blue water as dark object in NIR region. The deep water pixel was identified by finding the minimum radiance value in NIR region. Assuming the water contribution is negligible, the radiance measured is contributory sum of Rayleigh radiance and aerosol radiance. Rayleigh contribution was calculated using sensor geometry and aircraft altitude. The remaining is aerosol contribution which was used to calculate aerosol optical thickness (AOT). Assuming the atmosphere is uniformly distributed and AOT remains same over the reef, the path radiance contribution was removed. The calculated water leaving radiance is then divided by incoming solar irradiance to calculate the remote sensing reflectance of the surface. Figure 2 shows *in-situ* spectral signature of various benthic substrate. The spectral curves derived from atmospheric correction of AVIRIS-NG reflectance data very well matches with the in-situ spectral signature measured using ASD field spectroradiometer.

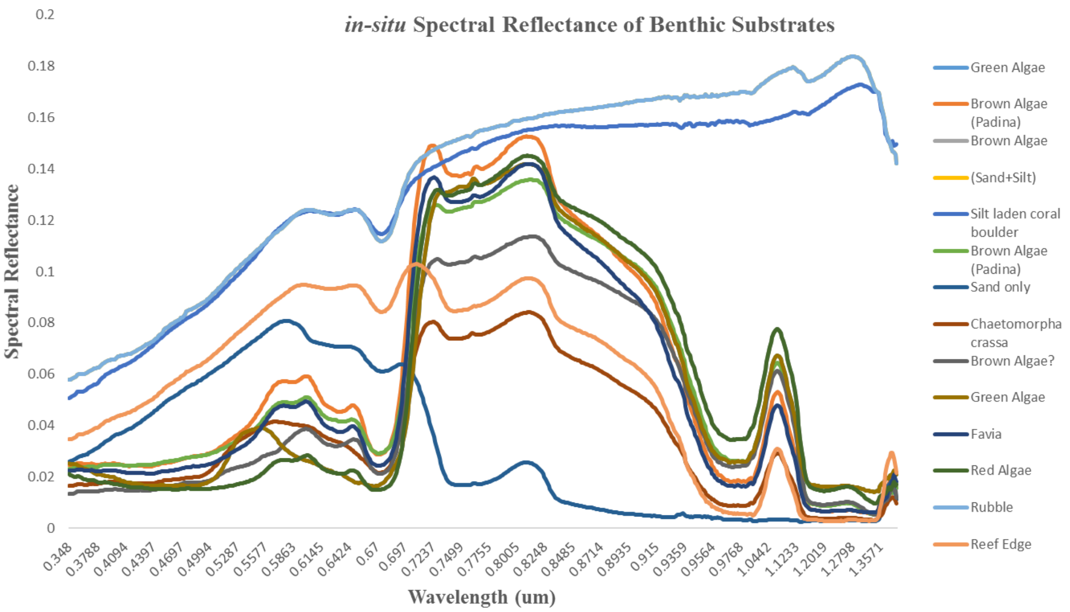

Figure 2*: in-situ* spectral signature of various benthic substrate

Exposed and water submerged substrate mask were created using difference of green and NIR reflectance channels. If reflectance in green channel is lower than reflectance in NIR channel then substrate is exposed and if reflectance in green channel is higher than reflectance in NIR channel then bottom substrate is overlaid with water column. The mask is applied to the image and water parameter inversion is then calculated over the masked pixels.

IOP inversion results simultaneously gave chlorophyll concentration, CDOM concentration, Suspended sediment concentration, water column depth over the submerged substrate pixels. A normalized value of all the parameters retrieved is shown in the figure 3. The chlorophyll concentration map shows high chlorophyll content near the algal rich zones of the reef. These regions are found mostly on the outer reef flat. CDOM was spread all over in the reef flat region. Suspended sediment concentration map shows water is clearer in the inner reef flat region. Turbidity increase on the reef shore where water interacts with the reef and churns heavily causing high suspended concentration in these regions. The bottom albedo map shows higher values over sand dominated fractional coverage over algae. The reef bottom topography is very well retrieved shown in water height map. Value of water height is less than 50 cm in the reef and increases off shore. Water logged area and shallow water region near the centre of the reef matches with the in-situ measurements.

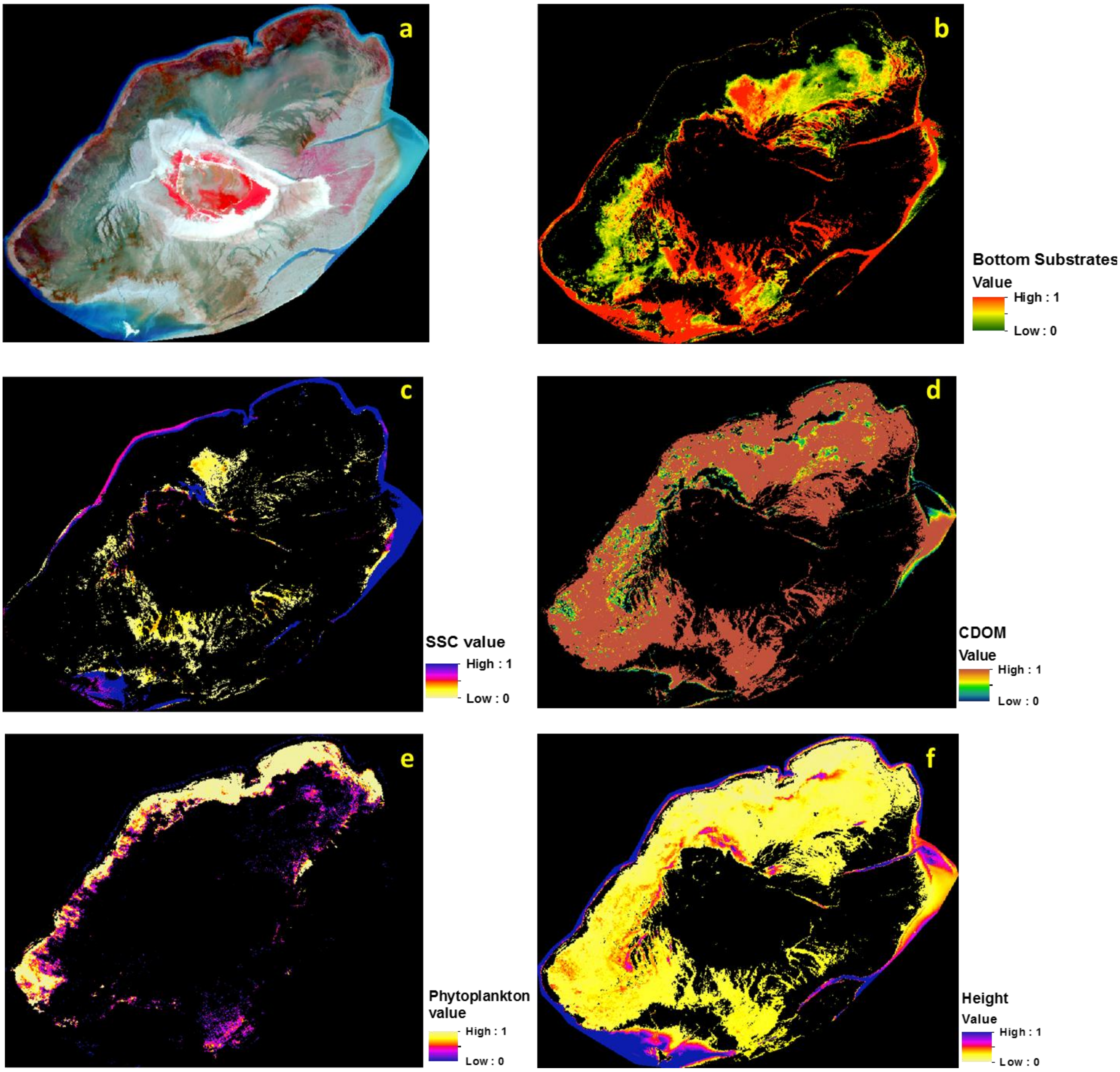

Figure 3: (a) Pirotan Image; normalized (b) Bottom substrates, (c) Suspended Sediment Concentration (SSC), (d) Coloured Dissolved Organic Matter (CDOM), (e) Phytoplankton, and (f) Water height determined using IOP inversion method.

The water quality parameters were used to calculate the diffuse attenuation coefficient (DAC) of overlaying water. The DAC and water height were used to calculate the effect of water column that changes the spectral signature of the bottom substrate. The water column correction plays an important role in determining the reflectance value of bottom. Deeper substrate has lower reflectance values as compared to shallow water as water mainly has an absorbing nature in NIR region. After water column correction, the albedo values for a particular bottom type were equal to each other irrespective of their depths. The reflectance image without water column correction and with water column correction was then classified using Spectral Angle Mapper (SAM). The results obtained is shown in figure 4.

SAM classification was performed based on spectral signatures collected from the image. The spectral signature location was chosen based on in-situ spectral signature and uniformity of area to classify it as end member spectra. SAM identifies the various classes in the image based on the calculation of the spectral angle. These classes were grouped into 10 major classes: Sand, deep water, shallow water, mangroves, mixed algae, brown algae, green algae, silt, sand with sparse algae and Rubble. The classification accuracy was estimated based on 52 in-situ locations spread over the reef. The classification accuracy of image without water column correction was 64.7 % which improved to 74.5 % after water column correction.

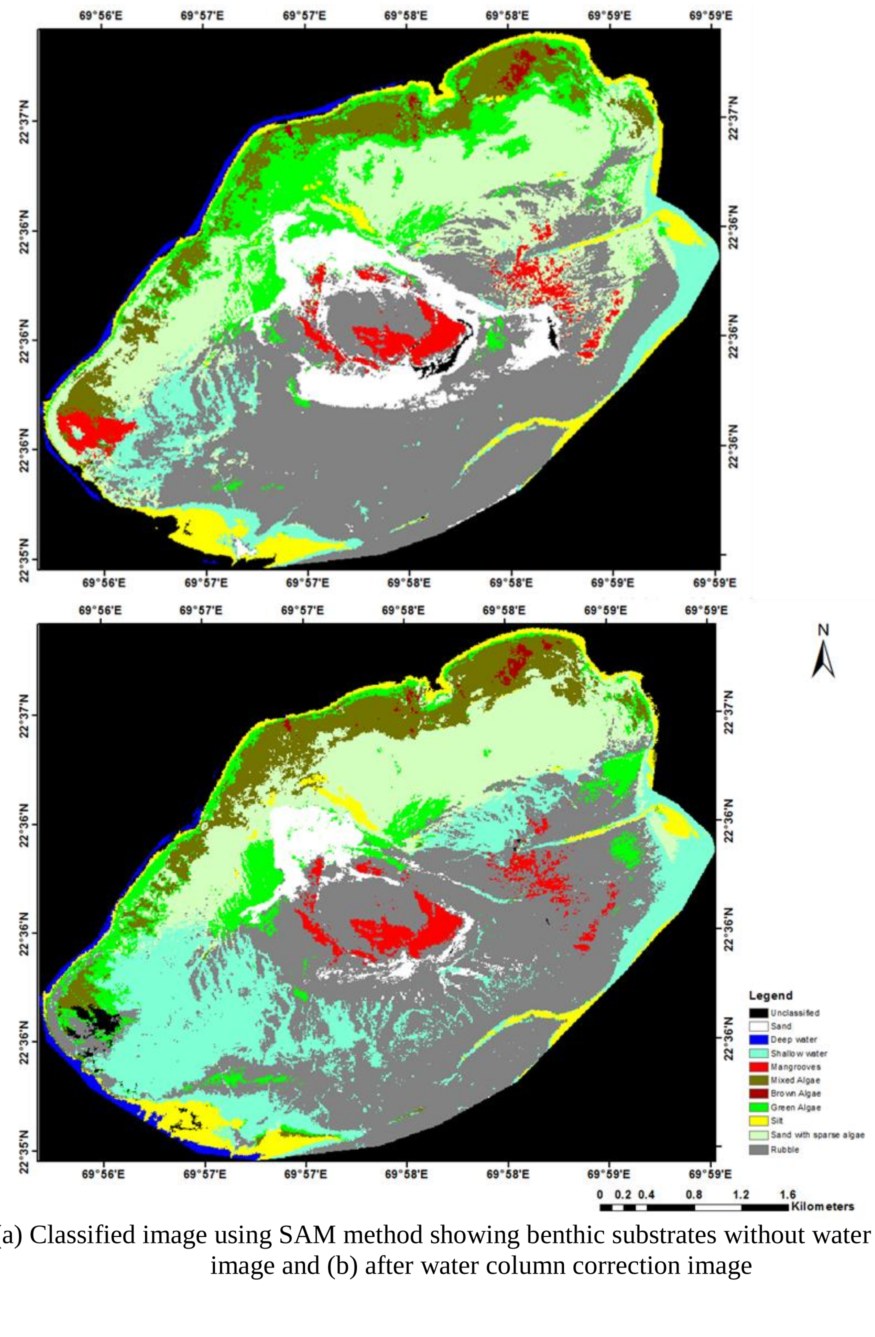

Figure 4: (a) Classified image using SAM method showing benthic substrates without water column correction image and (b) after water column correction image

CONCLUSION:

Physics based IOP inversion to estimate water quality parameters can be used in many types of water. The inversion results simultaneously give many water quality parameters which is better than empirical based inversions. The simultaneously retrieved bottom topography take care of bottom effects while inversion hence the results are very accurate. The effect of water plays a major role in altering the spectral signature hence water column correction is very important for generating the benthic coverage maps of coral reef environment.

ACKNOWLEDGMENT:

The authors are thankful to Shri Tapan Misra, Director, Space Applications Centre (SAC), Indian Space Research Organisation (ISRO) for his overall guidance and programme support. The authors acknowledge the guidance and support from Dr. Raj Kumar, Deputy Director, Earth, Ocean, Atmosphere and Planetary Sciences and Applications Area (EPSA), SAC. The authors express thanks to Dr. R. P. Singh, Head, Land Hydrology Division (LHD) and Ms. Nandani Ray Choudhury, Scientist SE, SAC for his constant encouragement and support. The authors extremely thankful to Marine National Park Authority at Jamnagar, Gujarat for giving permission to do field work in the region.

REFERENCES:

Brando, V. E., & Dekker, A. G. 2003. Satellite hyperspectral remote sensing for estimating estuarine and coastal water quality. IEEE transactions on geoscience and remote sensing, 41(6), 1378-1387.

Brando, V.E., Dekker, A.G., Park, Y.J., & Schroeder, T. 2012. Adaptive semianalytical inversion of ocean color radiometry in optically complex waters. Applied Optics, 51(15), 2808–2833.

Bricaud, A., Morel, A., Prieur, L., 1981. Absorption by dissolved organic matter of the sea (yellow substance) in the UV and visible domains. Limnology and Oceanography 26 (1), 43–53.

Bucholtz, A. 1995. Rayleigh-scattering calculations for the terrestrial atmosphere. Applied Optics, 34(15), 2765-2773.

Buiteveld, H., Hakvoort, J. M., & Donze, M. 1994. The optical properties of pure water. *Ocean Optics XII, Proc.SPIE 2258*, 174-183.

Gege, P. 2012. Analytic model for the direct and diffuse components of downwelling spectral irradiance in water. Applied Optics, 51(9), 1407–14019.

Gege, P. 2014. WASI-2D: A software tool for regionally optimized analysis of imaging spectrometer data from deep and shallow waters. *Computers & Geosciences, 62*, 208-215.

Giardino, C., Candiani, G., Bresciani, M., Lee, Z., Gagliano, S., & Pepe, M. 2012. BOMBER: A tool for estimating water quality and bottom properties from remote sensing images. Computers & Geosciences, 45, 313-318.

Giardino, C., V. E. Brando, A. G. Dekker, N. Strombeck, and G. Candiani. 2007. Assessment of water quality in Lake Garda (Italy) using Hyperion. *Remote Sensing of Environment* 109 (2): 183-195.

Gordon, H. R., 1997. Atmospheric correction of ocean color imagery in the Earth Observing System, Journal of Geophysical Research, 102 (D14), pp. 17081-17106.

Heege, T., 2000. Flugzeuggestu¨ tzte Fernerkundung von Wasserinhaltsstoffen im Bodensee. Dissertation, DLR-Forschungsbericht 2000-40, 141pp.

Kou, L., Labrie, D., & Chylek, P. 1993. Refractive indices of water and ice in the 0.65-to 2.5-µm spectral range. Applied optics, 32(19), 3531-3540.

Kutser, T., Miller, I., & Jupp, D. 2006. Mapping coral reef benthic substrates using hyperspectral space-borne images and spectral libraries. Estuarine, Coastal and Shelf Science, 70, 449-460.

Lee, Z., Carder, K., & Arnone, R. 2002. Deriving inherent optical properties from water color: A multiband quasianalytical algorithm for optically deep waters. *Applied Optics, 41*, 5755-5772.

Lu, Z. 2006. Optical Absorption of Pure water in the blue and ultraviolet. Ph.D. Thesis, A&M University, Texas.

Maritorena, S., Morel, A., & Gentili, B. 1994. Diffuse reflectance of oceanic shallow waters: Influence of water depth and bottom albedo. Limnology and Oceanography, 39(7), 1689-1703.

Morel, A., 1995. Optical modeling of the upper ocean in relation to its biogenous matter content (case 1 waters), J. Geophys. Res. 93, 10,749-10,768,

Mumby, P. J., Clark, C. D., Green, E. P., & Edwards, A. J. 1998. Benefits of water column correction and contextual editing for mapping coral reefs.International Journal of Remote Sensing, 19(1), 203-210.

Navalgund, R.R., Ajai, Bahuguna, A., Ray Chaudhury, N., Bhattji, N.S., Madhupriya, N., Sharma, S., Parihar J. S., Panigrahi, S., Chakraborty, M., Dwivedi, R. M., Ramdass, S. and Swaroop, P. 2010. Coral Reef Atlas of the World Vol.1 Central Indian Ocean, Space Applications Centre, (ISRO), Ahmedabad, 282p.

Nyquist, G., 1979. Investigation of some optical properties of seawater with special reference to lignin sulfonates and humic substances. Dissertation, Go¨ teborgs Universitet, 200pp.

Odermatt, D., Gitelson, A., Brando, V.E., & Schaepman, M. 2012. Review of constituent retrieval in optically deep and complex waters from satellite imagery. Remote Sensing of Environment, 118, 116–126.

Pope, R. M., & Fry, E. S. 1997. Absorption spectrum (380–700 nm) of pure water. II. Integrating cavity measurements. Applied optics, 36(33), 8710-8723.

Salama, M. S., & Verhoef, W. 2015. Two-stream remote sensing model for water quality mapping: 2SeaColor. Remote Sensing of Environment, 157, 111-122.

Venkataraman, K., Coral reefs of India. In: (Hopley D. ed) Encyclopaedia of modern coral reefs. Springer, 2011, pp. 267-275.